AVCO EVERETT RESEARCH LABORATORY

a division of
AVCO CORPORATION

MAGNETIC RADIATION SHIELDING SYSTEMS ANALYSIS

R. E. Bernert and Z. J. J. Stekly

SUPERCONDUCTING COIL TECHNOLOGY

E. D. Hoag and Z. J. J. Stekly

AMP 134
Contract NAS 8-5278
July 1964

prepared for

GEORGE C. MARSHALL SPACE FLIGHT CENTER
NATIONAL AERONAUTICS AND SPACE ADMINISTRATION

AMP 134

MAGNETIC RADIATION SHIELDING SYSTEMS ANALYSIS

by

R. E. Bernert and Z. J. J. Stekly

and

SUPERCONDUCTING COIL TECHNOLOGY

by

E. D. Hoag and Z. J. J. Stekly

AVCO-EVERETT RESEARCH LABORATORY
a division of
AVCO CORPORATION
Everett, Massachusetts

July 1964

Contract NAS 8-5278

prepared for

GEORGE C. MARSHALL SPACE FLIGHT CENTER
NATIONAL AERONAUTICS AND SPACE ADMINISTRATION
Huntsville, Alabama

FOREWORD

These summary papers were presented at the Electromagnetic Shielding Conference held at the George C. Marshall Space Flight Center, National Aeronautics and Space Administration, Huntsville, Alabama on January 27, 1964.

MAGNETIC RADIATION SHIELDING SYSTEMS ANALYSIS

by

R. E. Bernert and Z. J. J. Stekly

ABSTRACT

33858

An analytic program to study the feasibility of Superconducting Magnetic Radiation Shielding was begun at Avco-Everett Research Laboratory under NASA Contract in 1963. The object of the program is to investigate different magnetic field configurations as possible shield geometries and to determine the shielding effectiveness and system mass of each configuration. This paper summarizes the analytical approach and presents some preliminary results of the progress to date.

author

SUPERCONDUCTING COIL TECHNOLOGY

by

E. D. Hoag and Z. J. J. Stekly

ABSTRACT

The state-of-the-art of Superconducting Coil Technology is such that large, high field strength magnets have not yet been built. The largest coils built so far have been constructed at Avco-Everett Research Laboratory from .010-inch diameter Nb-Zr wire, achieving 18,000 gauss with an energy storage of 70,000 joules. The effort at AERL to advance the state-of-the-art has been concerned with theoretical and experimental studies of both wire and strip material. It has proceeded mainly in two areas, determination of the properties of superconducting materials, and the behavior of superconducting coils. In the work under NASA sponsorship the properties of Nb-Zr strip have been studied in detail and a coil has been constructed from the same material.

author

MAGNETIC RADIATION SHIELDING SYSTEMS ANALYSIS

by

R. E. Bernert and Z. J. J. Stekly

Introduction

The relative advantage of employing a magnetic shield in lieu of a bulk-type shield may be determined by comparing the mass requirement for each which limits the dose rate within a given volume to a specified level. In order to determine the effect of field geometry on the mass requirement, three field geometries have been investigated. For each of the geometries considered, the major components are:

Superconducting Wire
Support Structure
Cryogenic Environment

General expressions for each of these have been determined and an optimization procedure carried out to minimize the total weight of the shield system. The minimum can then be compared with passive shield weights.

Field Geometries

The three field geometries considered are shown in Fig. 1. Two arrangements have confined magnetic fields while the third is an external field dipole.

I. Unconfined Field Dipole

The unconfined field configuration is toroidal in shape similar to a ring shaped hollow conductor. Placing the windings at the outer limit of the shielded region formed by the field, produces a desirable shielded region of relatively low field. Several authors have investigated the extent of the shielded region including Levy,[1] whose analysis has been used in this study.

Considering the geometry in Fig. 1, the J x B force on the winding is compressive, requiring that the winding be supported with a surface structure. The mass of the structure is found by considering both the tangential and meridional forces on the geometry. This was accomplished by using the analysis of Stekly[2] for a toroidal conductor.

To maintain the coil at superconducting temperatures, the winding would be refrigerated via refrigeration coils and insulation applied to both the exterior and interior surface of the torus.

Should field leakage into the shielded region be too high, additional windings may be provided to reduce or eliminate the field from the shielded volume with some increase in weight.

II. Confined Field Geometries

A. Double Torus

The confined field double torus consists of two toroidal windings, one inside the other. The general arrangement is shown in the lower left of Fig. 1. Current direction on the inner winding is opposite to that on the outer winding providing a field free shielded region within the inner torus.

In this geometry, the field intensity decreases with distance from the origin. This field variation requires that the two windings be eccentric with respect to each other in order to shield from all directions all particles up to the specified design energy. Thus the Larmor radius for a given proton energy is greater on the outer portion where the field intensity is lowest.

Structural support must be provided for both windings. Now the "magnetic pressure" exerts a compressive force on the inner winding and an internal pressure on the outer winding. The inner winding may be supported from the outer winding by means of tension members indicated on the figure as support structure.

The outer winding must also be provided with structural support whereever the magnetic forces result in stresses above the allowable of the wire. A constant-stress surface structure has been calculated which yields a toroid of variable shell thickness.

To maintain the windings at superconducting temperature, refrigeration is supplied between the windings and insulation applied on the outer surface of the outer winding and the inner surface of the inner winding.

B. Hybrid Torus

The second confined field geometry can be generated by deforming a toroidal winding as shown in the lower right of Fig. 1. The shielded region is spherical in shape and is located in the center of the geometry. For this configuration it is necessary to add a polar plug of passive shielding material to prevent proton leakage at the field interface.

The field is generated by a single toroidal winding indicated in the figure and is confined within the winding providing a field free shielded region. To eliminate field variation at a given radius from the center of the sphere, a winding of constant thickness is provided by crossing wire through the field such that the total conductor cross-section is greatest at the equator and essentially zero at the poles. This procedure eliminates high fields at the poles. It also permits the field depth to be constant for a given design proton energy.

Structural support for the magnetic forces is provided much the same as that for the double torus. An important difference however, is that the total force acting to expand the outer winding is equal and opposite to the force

tending to compress the inner winding. This being the case, a support structure comprised of a system of tension hoops can be provided between the inner and outer windings, shown as support structure in Fig. 1. Additional support is required for the crossover wire.

At the poles of the shield, particles are either curved toward or away from the pole centerline. When the particle is curved toward the centerline there is the possibility that particles of lower than design energy can penetrate the field. If particles of a given charge are curved toward one pole of the shield, they will be curved away from the opposite pole. Since the shield is designed primarily for positively charged protons it is, therefore, necessary to cap (plug) only one pole of the shield.

The geometry of the plug has been calculated to prevent leakage of all protons up to the design energy. The general shape is shown in Fig. 1. It has a thickness along the pole centerline sufficient to completely stop the design proton and tapers to zero at a distance from the centerline equal to slightly less than one Larmor diameter. Polyethylene has been used in the calculations as the plug material.

Maintaining the windings at superconducting temperatures is accomplished in the same manner as for the double torus.

Cryogenic Environment

The mass required to provide the low temperature environment for a superconducting magnetic shield is comprised of insulation and a refrigeration source which includes machinery, shaft power and heat rejection radiator. This approach has been found to be lighter than a stored helium system primarily because of the extended mission times anticipated for magnetic shield applications.

After determining:

1) the specific mass and efficiencies of advanced types of refrigerators for superconducting temperatures,

2) the effectiveness and density of superinsulation materials,

3) the specific mass of space power systems, and

4) the specific performance of space radiators,

a mass optimization was carried out to estimate the mass requirement to provide the refrigeration in space. The results are shown as a function of the insulated surface area in Fig. 2. It should be pointed out that these results are based on advanced refrigerators now in the component development stage and on space power system specific masses varying from 45 kg/kW at

10 kW output to 5 kg/kW at 1000 kW output.[3] The figure also shows the effect of employing LH_2 propellant as a radiation barrier. No penalty is taken for heat added to the propellant.

Mass Optimization Procedure

With expressions derived for the mass of the major components of the shield system, optimization calculations can be made for each of the three geometries studied. The essential steps to the procedure are shown in Fig. 3. The volume to be shielded and proton energy level are specified in addition to the physical properties of the materials to be used. Maximum field strength, current density and the strength to weight ratio of the structure are the predominating factors. Note that superconductors have critical fields and current densities above which they cannot operate as superconductors. Therefore limits are set for these properties. Next, for a given field geometry the mass of wire and structure are calculated as a function of field strength. There is an optimum field strength which will yield a minimum mass of structure and wire. In addition, since the surface area is also a function of the field strength, the three components may be plotted for minimum system mass.

Figure 4 shows a typical variation of the weights of the individual components for a hybrid torus. Note for the hybrid that the mass of the polar plug is also required and becomes more important at the lower field intensities.

The optimum shown on the figure is at approximately 45 kilogauss. The figure also shows that for this case the system mass is most sensitive to changes in the current carrying capacity of the wire. For other cases and geometries, other components predominate.

The variation of shield mass with shielded volume for the three geometries is plotted in Fig. 5. Also shown on the figure is the mass of a spherical passive polyethylene shield. The results shown in the figure indicate that the hybrid geometry yields the lowest shield weight of the three magnetic geometries and that the weight of the magnetic shields increases with volume at a lower rate than the passive shield.

It should also be pointed out that the external field geometry tends to optimize for small cross sections of the shielded region.

A minimum cross section was taken as a circle having a radius of 0.38 meters or 15 inches. This limit is probably small for extended missions and will exclude the external dipole geometry from consideration for some combinations of shield requirements and material properties.

Magnetic and Passive Shield Comparison

Passive polyethylene spherical shields are compared with the magnetic hybrid geometry in Fig. 6. Note that at 100 MeV the passive shield appears to be superior to the magnetic shield, while from about 100 to 170

MeV (depending on volume) the magnetic shield shows weights below the passive shields.

Dose Rate Considerations

Dose rates for passive and magnetic shields will be different for a given design threshhold level. This is true for both primary and secondary contributions to the total dose.

The main difference is the fact that no secondaries are produced by the interaction of the protons with a magnetic field. Hence, for the external field dipole, the only secondaries produced are those resulting from the high energy (low intensity) end of the flare spectrum passing through the winding. For the confined field types, secondaries are produced in the outer winding much the same as for passive shields, except that less mass is available.

Differences in the primary dose also exist. The proton spectrum passing through a passive shield suffers a greater energy decay than if it had passed through a magnetic shield. Since dose is a function of the linear energy transfer rate (LET) which varies with energy, the energy absorbed by the target will differ for the two shields. In general, the primary dose for a magnetic shield will be below the passive shield dose. This dose comparison will be one of the results of the analysis now being conducted.

Conclusion

The analysis of magnetic shield systems for proton shielding using superconducting coils indicates that the magnetic shield approach could be promising for shielding levels above 200 MeV.

REFERENCES

1. Levy, R., "Radiation Shielding of Space Vehicles by Means of Superconducting Coils," Avco-Everett Research Laboratory Research Report 106, April 1961.

2. Stekly, Z. J. J., "Magnetic Energy Storage Using Superconducting Coils," Avco-Everett Research Laboratory AMP 102, January 1963.

3. Bernatowicz, D. T., Guentert, D. C., Klann, J. L., "Space Powerplant Needs and Selection," Astronautics and Aerospace Engineering, 1, 22-26, May 1963.

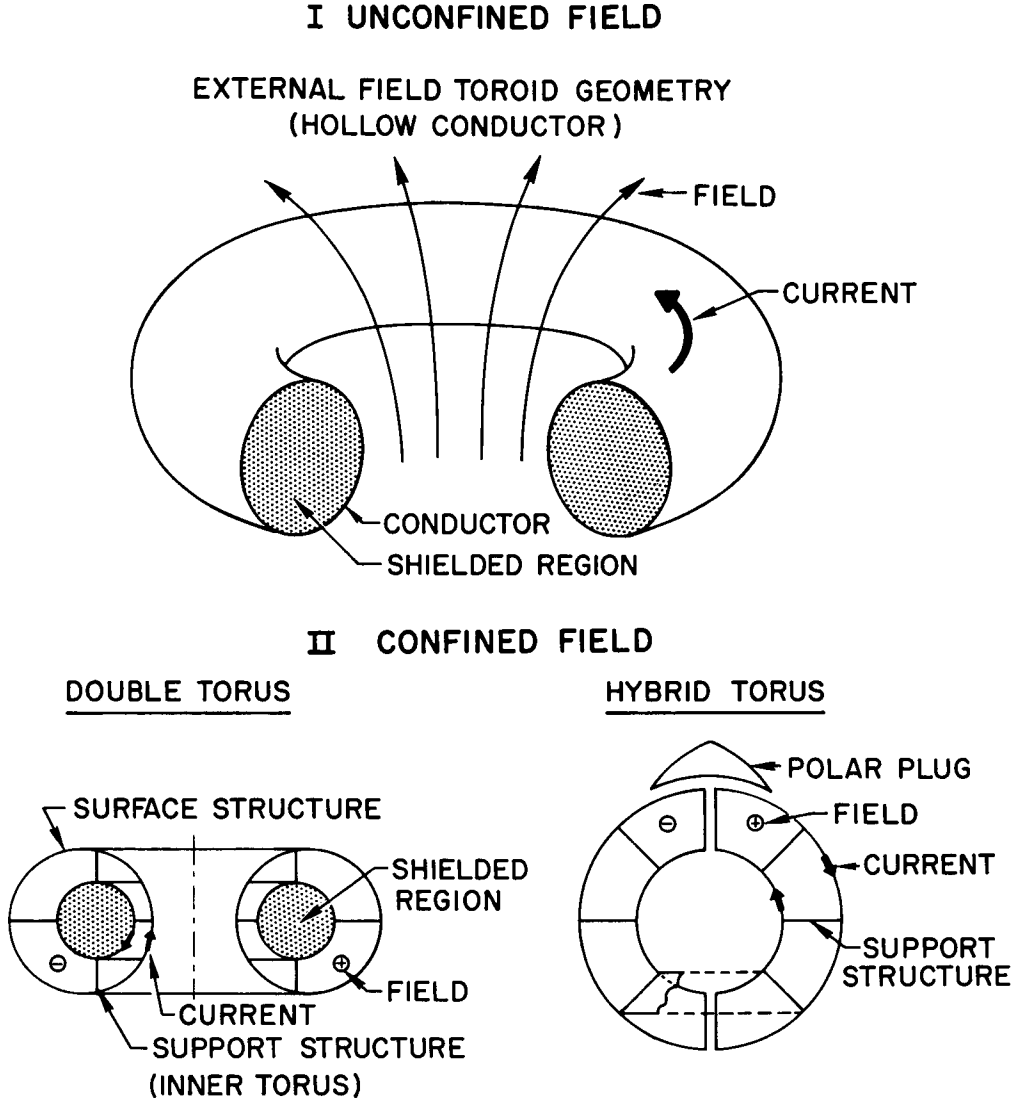

Fig. 1 Magnetic Field Configurations.

A1857

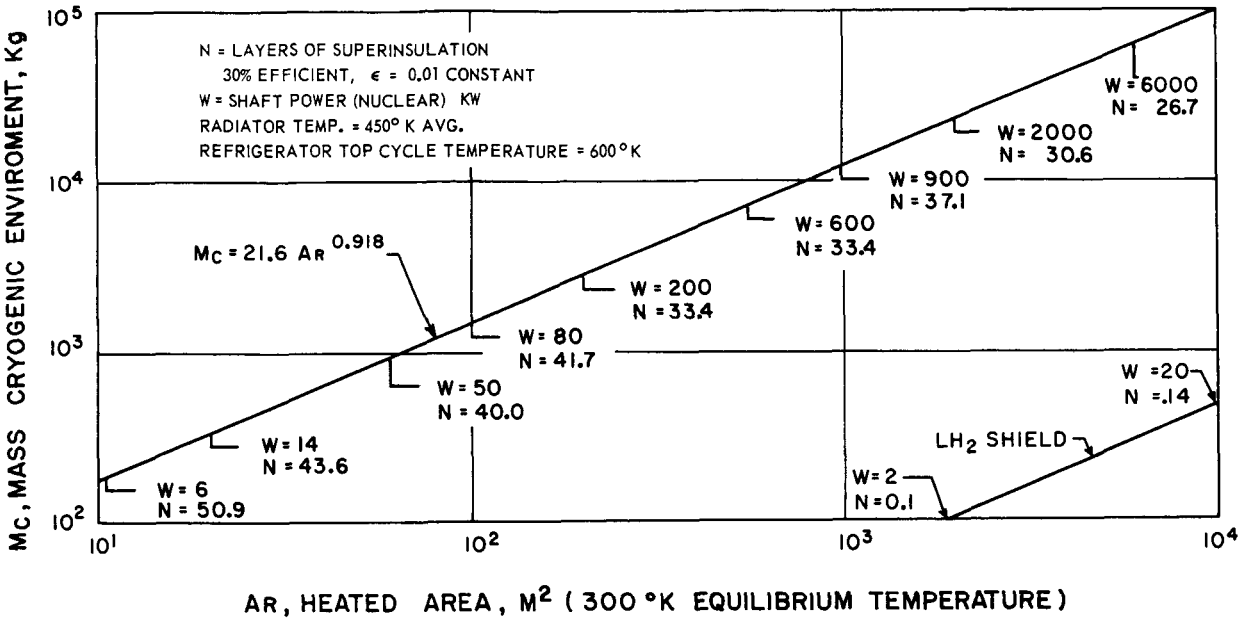

Fig. 2 Plot showing the mass requirement to maintain 4.2°K in space. The system is comprised of insulation, refrigerator, power source and heat rejection radiator.

I. INPUT DATA

1. Volume to be Shielded
2. Shielding Level
3. Material Properties

II. SELECT FIELD CONFIGURATION

III. CALCULATE

1. Mass of wire and structure as function of B_{max}
2. Add weight of cryogenic environment previously optimized as a function of surface area
3. Optimize sum of wire, structure and cryogenic with respect to B_{max} for minimum mass and optimum geometry

Fig. 3 Mass Optimization Procedure used to determine Minimum System Weight.

A1757

A1858

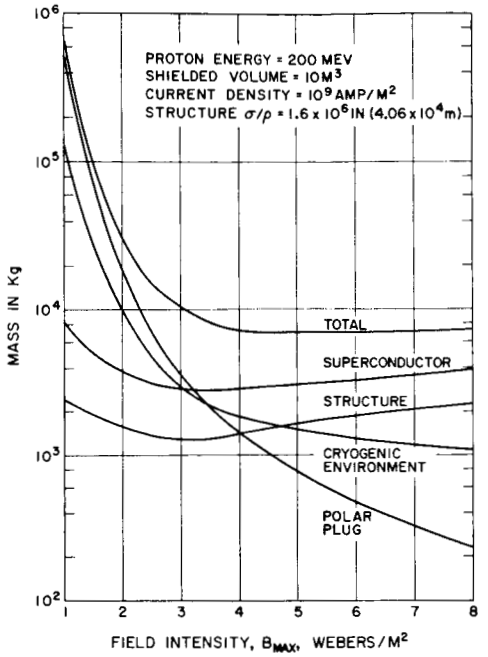

Fig. 4 Plot showing the relation among component weights for a hybrid torus geometry magnetic shield.

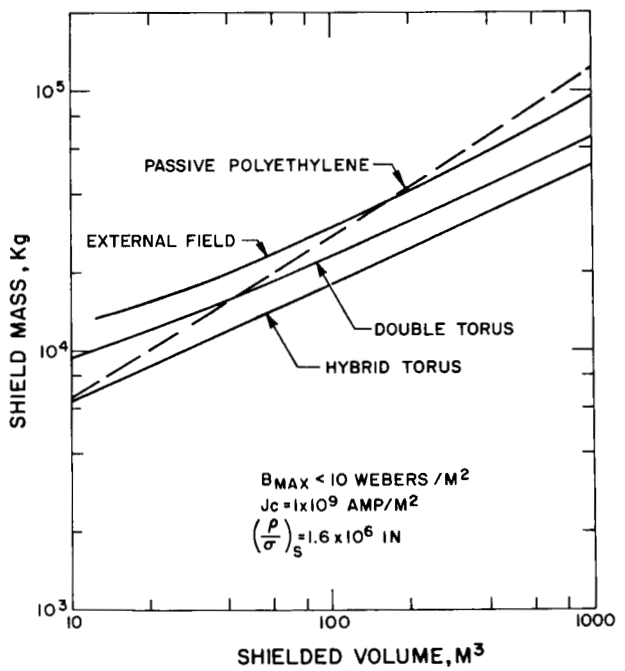

Fig. 5 Plot comparing passive and magnetic shield weights vs shielded volume for a shielding level of 200 MeV.

A2044

A1860

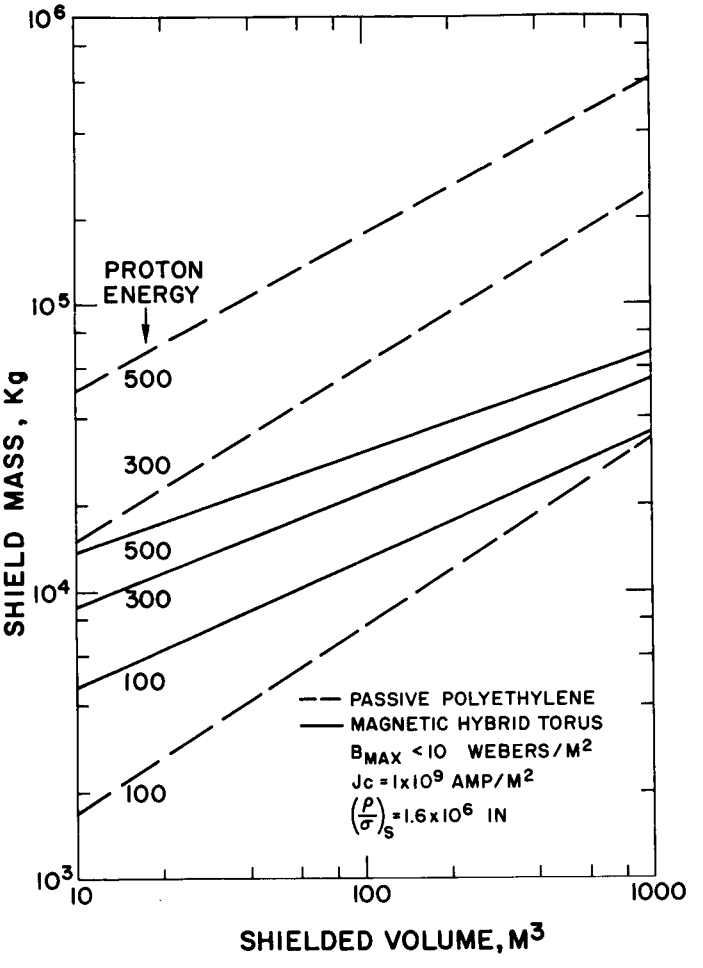

Fig. 6 Plot of passive polyethylene and magnetic hybrid shields vs shielded volume for several shielding levels.

A1861

SUPERCONDUCTING COIL TECHNOLOGY

by

E. D. Hoag and Z. J. J. Stekly

Superconducting Coils

The state-of-the-art of superconducting coils is summarized in Fig. 7, which shows the magnetic field at the center versus diameter which has been achieved. It is very evident from the figure that large high field strength coils have not yet been built. The reason for this is a combination of the high cost of superconducting materials coupled with the fact that the difficulty of building coils increases with increasing energy stored in the magnetic field.

The large coils that have been built so far utilized mainly Nb-25% Zr and NB-33% Zr .010-inch diameter wire. Figure 8 shows the largest superconducting coil built so far. It consists of 12 spools, 6 inner ones and 6 outer ones. The inner ones are wound with Nb-33% Zr .010-inch diameter copper plated wire, and the outer ones of Nb-25% Zr. 010-inch diameter copper plated wire. This magnet system contains about 120 miles of superconducting wire connected in series. As of this date the coil system has achieved 18,000 gauss using 2 inner coils and 2 outer coils corresponding to a magnetic energy storage of 70,000 joules. The completed twelve coil set shown in Fig. 8 is now in the process of being tested.

This type of construction results in a high inductance and leads to very high voltages during a transition to the normal state. Further, the use of small diameter wire in series could result in one bad section of wire limiting the whole coil performance.

The superconducting programs at Avco-Everett Research Laboratory, including the work sponsored by NASA are aimed at:

1) Determination of the properties of Superconducting Materials.

2) Study of coil effects, namely:

   a) Transition to the normal state must be fully understood for two reasons: (1) To protect the magnet from damage. (2) If any type of stabilization is attempted, this cannot be done without a thorough understanding of the process.

b) Achieving designability - the main problem with coils being built with superconducting alloys is that the current carrying capacity in a coil is considerably less than that in a coil made of the same material - this departure from short sample behavior must be fully understood before large coils can be successfully designed.

c) Stability of Operation - the ideal superconducting coil would recover from a severe disturbance, with little loss in field strength. This type of operation can only be achieved by a complete knowledge of the phenomena involved.

Under the program sponsored by NASA, our aim is first to determine the properties of superconductors of strip geometry in short samples, and to correlate these with coil performance.

The emphasis is on strip, since for the large coils contemplated for use in Radiation Shielding it is necessary to develop conductors of cross-section larger than the .010-inch diameter wire now in use.

One of the unique properties of strip which sets it apart from wire is its anisotropy with respect to magnetic field. A typical example of this is shown in Fig. 9 where critical current density can be seen plotted as a function of the angle between the magnetic field and plane of the strip (current direction is perpendicular to magnetic field).

Another interesting property of strip is the way in which magnetic field penetrates and becomes trapped. Figure 10 shows photographs taken by means of a magneto-optic device which actually forms an image corresponding to flux penetrating the strip. The device consists of a second surface mirror of magneto-optic glass placed directly in contact with a thin strip sample in a perpendicular magnetic field. A light source and optical system employing crossed polarizers are then used to form an image which varies in intensity and color in a way which can be interpreted in terms of field intensity.

The first picture of the sequence shows the strip with flux already trapped. Subsequent pictures show the motion of this flux as the external field is taken through a complete cycle. The field plots beneath each picture shows qualitatively the normal component of the total field at the surface of the strip.

In order to correlate some of the short sample behavior with actual coil performance, a strip coil has been constructed. This coil, shown in Fig. 11, contains various probes and other instrumentation to test its stability to electrical, thermal and mechanical perturbation. In initial tests it has produced approximately 5 kilogauss at 75 amperes in the persistent mode. This does not represent its limit however, and other tests are planned in the near future.

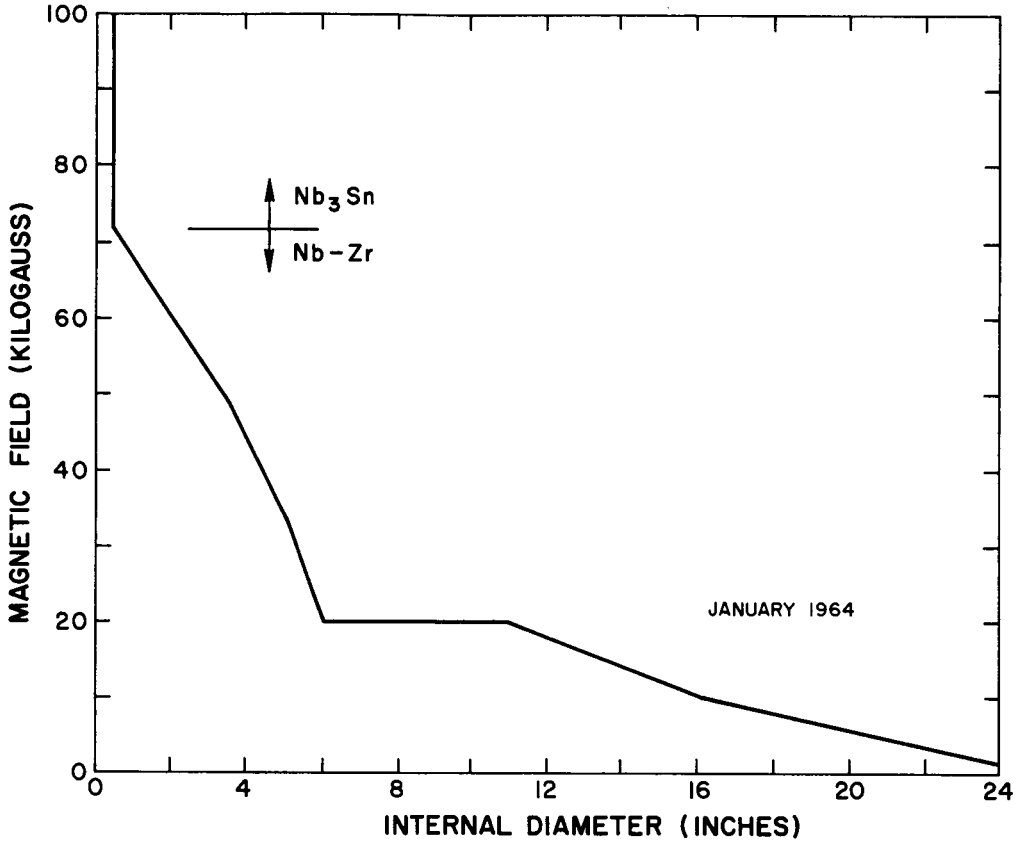

Fig. 7 State-of-the-art of Superconducting Coil.

A1167

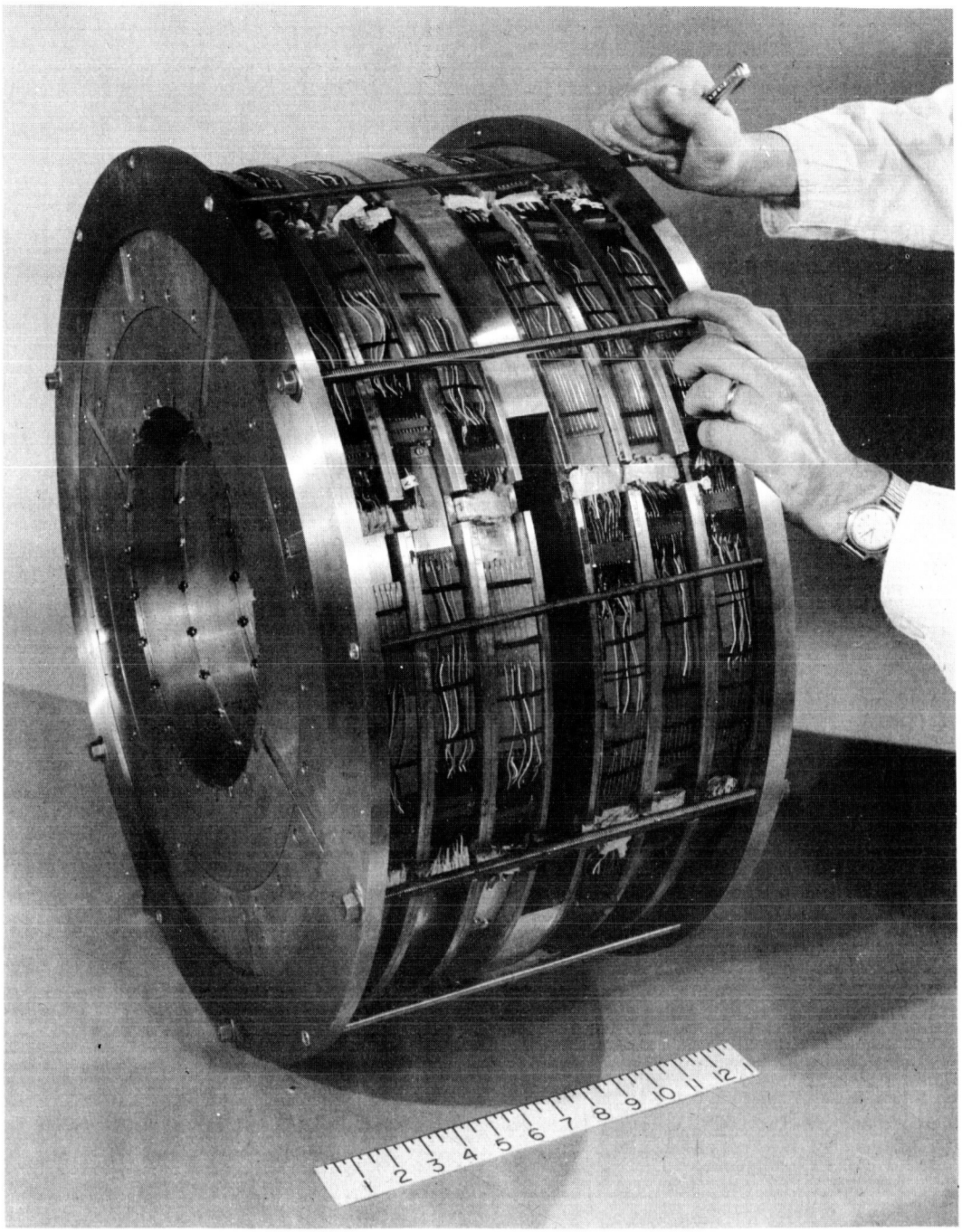

Fig. 8 Argonne Coil System.

A1854

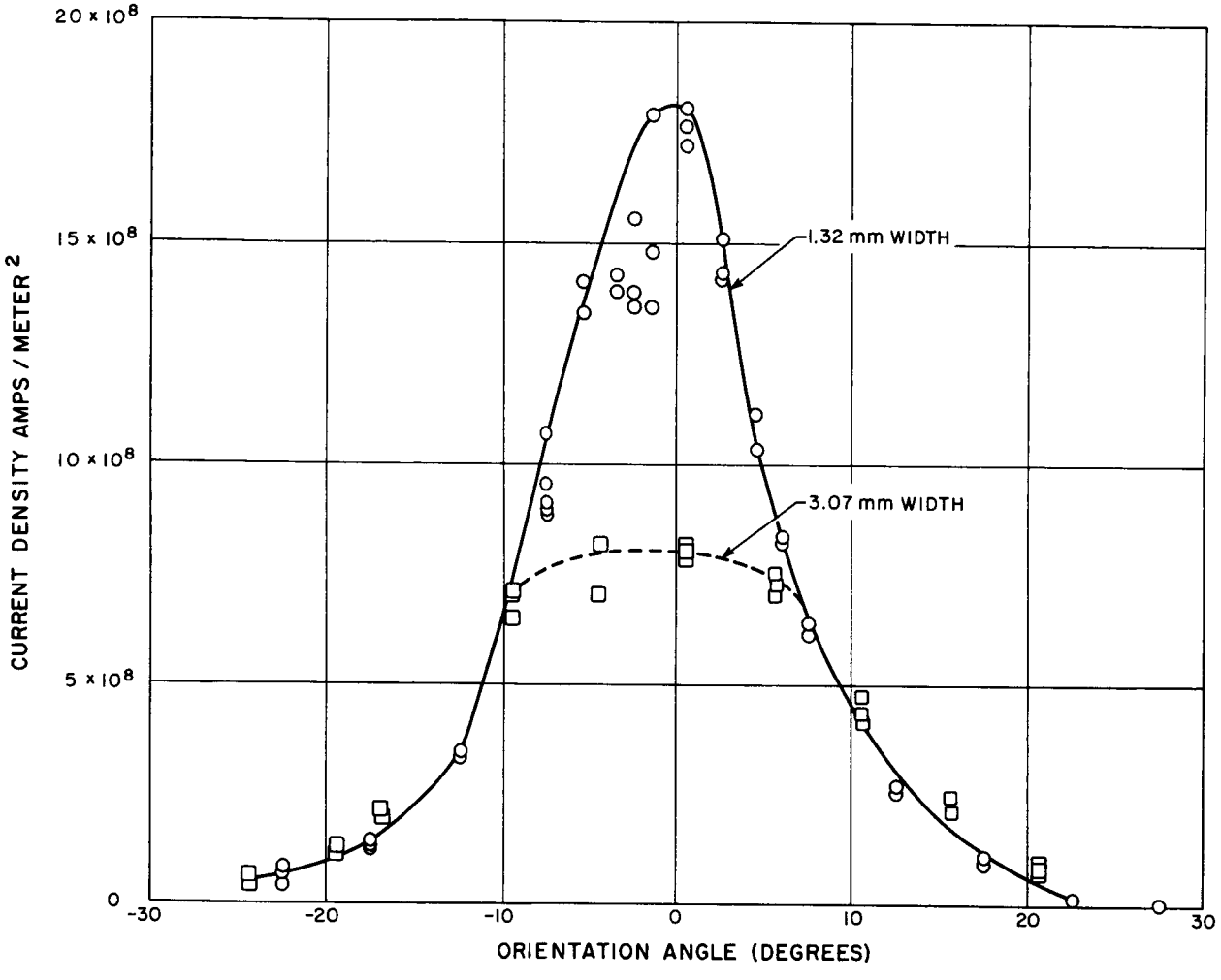

Fig. 9 Niobium Zirconium Strip Characteristic.

A1769

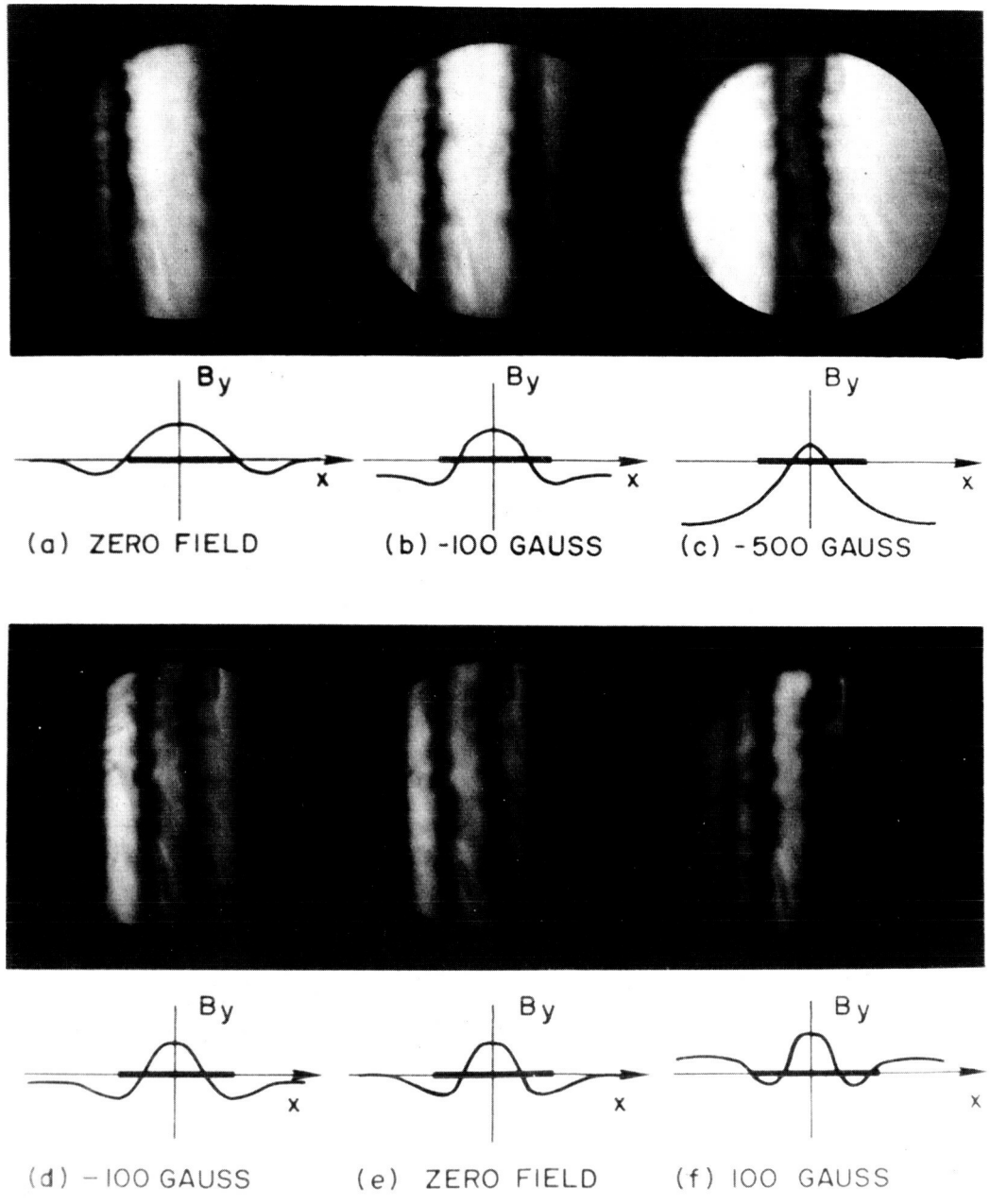

Fig. 10 Flux Trapping in Niobium Strip.

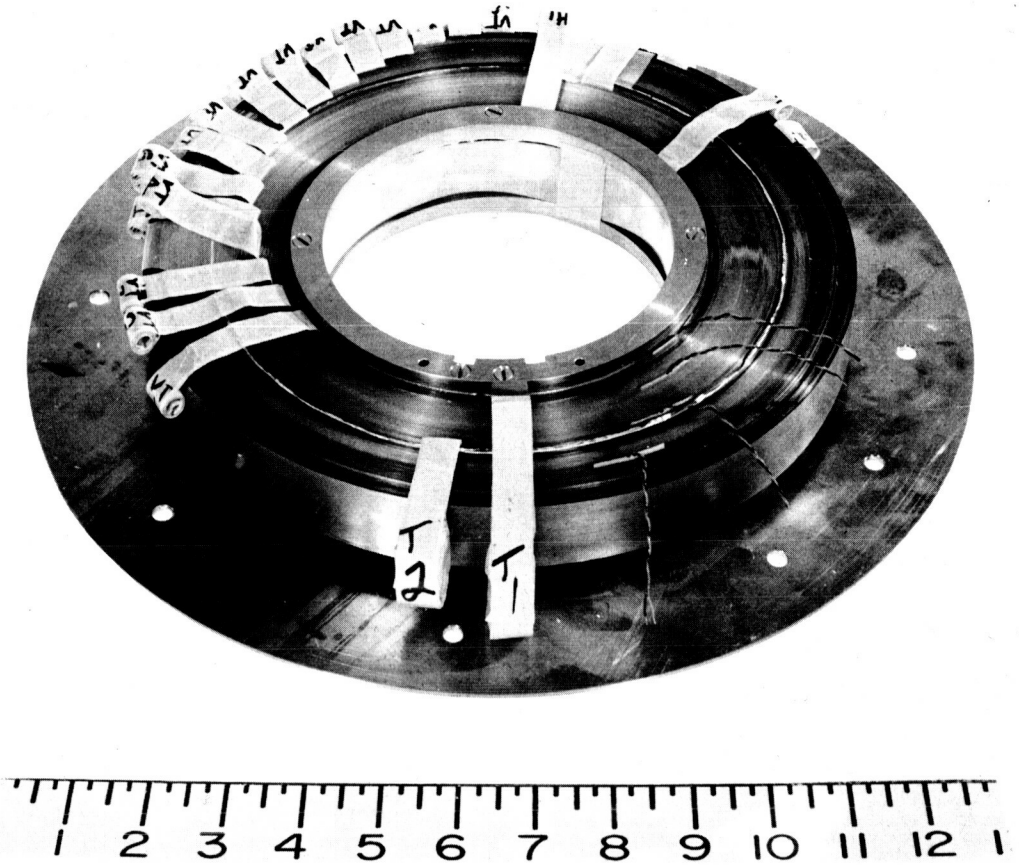

Fig. 11 Experimental Strip Coil.

A1852